*Transactions*, SMiRT-24
BEXCO, Busan, Korea - August 20-25, 2017
Division IX (include assigned division number from I to X)

# CREEP DAMAGE EVALUATIONS FOR BWR LOWER HEAD IN SEVERE ACCIDENT

**Jinya Katsuyama[1], Yoshihito Yamaguchi[2], Yoshiyuki Nemoto[3], Yoshiyuki Kaji[4] and Masahiko Osaka[5]**

[1] Principal Researcher, Nuclear Science and Engineering Center, Japan Atomic Energy Agency, Japan
[2] Researcher, Nuclear Safety Research Center, Japan Atomic Energy Agency, Japan
[3] Assistant Principal Researcher, Nuclear Science and Engineering Center, Japan Atomic Energy Agency, Japan
[4] Senior Principal Researcher, Nuclear Science and Engineering Center, Japan Atomic Energy Agency, Japan
[5] Group Leader, Nuclear Science and Engineering Center, Japan Atomic Energy Agency, Japan

## ABSTRACT

It is difficult to assess rupture behavior of the lower head of reactor pressure vessel in boiling-water-type nuclear power plants due to severe accident like Fukushima Daiichi. One reason is that boiling water reactor (BWR) lower heads have geometrically complicated structure with a lot of penetrations. Another one is that BWR lower head is composed of various types of materials of RPV, weld-overlay cladding, control rod guide tubes, stub tubes, welds, etc. Therefore, we have been developing an analysis method to predict time and location of RPV lower head rupture of BWRs considering creep damage mechanisms based on coupled analysis of three-dimensional thermal-hydraulics (TH) and thermal-elastic-plastic-creep analyses. To conduct such analyses, we have continued to obtain experimental data on creep deformation in high temperature range. In this study, we performed creep damage evaluations based on developing analysis method by using detailed three-dimensional model of RPV lower head with control rod guide tubes, stub tubes and welds. Creep damage evaluation based on four types of damage criteria of "Considere", strain, Kachanov, and Larson-Miller-parameter (LMP) were made by using experimentally determined parameters. To investigate the effects of the debris depth and heat generation locations on failure behavior of lower head, we conducted parameter studies varying analysis conditions related to relocated molten core. From the analysis results, we discussed the outflow paths of the relocated molten core to the containment, and it was concluded that failure regions of BWR lower head are only the control rod guide tubes or stub tubes under simulated conditions.

## INTRODUCTION

After the Fukushima Daiichi (1F) nuclear power plant (NPP) accident due to the Pacific coast of Tohoku earthquake and Tsunami in March, 2011, Japan Atomic Energy Agency (JAEA) has been conducting various research activities for the early completion of the decommissioning of NPPs. Before the 1F accident, several researches regarding phenomena inside the reactor and failure behavior of the reactor pressure vessel due to severe accidents had been actively conducted in reaction to the Three Mile Island accident in 1979 (Onizawa, 1993), (Humphphries, 2002), (Tran, 2010), (Villanueva, 2011). However, it is difficult to assess rupture behavior of the lower head of RPV in boiling-water-type NPPs like 1F due to severe accident. One reason is that boiling water reactor (BWR) lower heads have geometrically complicated structure including a lot of penetrations with large diameter. Another one is that BWR lower head is composed of various types of materials of RPV, cladded weld-overlay, control rod guide tubes, stub tubes, welds, etc. Therefore, we have been developing an analysis method to predict time and location of rupture for RPV lower head of BWRs considering creep damage mechanisms based on three-dimensional thermal-hydraulics (TH) and thermal-elastic-plastic-creep analyses.

In the previous paper (Katsuyama, 2016), we developed finite element model of RPV lower head including penetrations, welds and core internals, and prepare several creep damage failure models to predict time and location of RPV lower head rupture. Structural response and failure behavior due to

heating by molten core was evaluated by coupled analysis of TH and structural analyses. In this paper, we improve the analysis model of BWR lower head, and parametric analyses are performed assuming the variations of relocation behavior of molten core and internals. The analysis codes used for the coupled analysis are FINAS/CFD (ITOCHU Techno-Solutions Corporation, 2013) and FINAS/STAR (ITOCHU Techno-Solutions Corporation, 2013). The behavior of molten core at the RPV lower head is evaluated by TH analysis. Using temperature distributions obtained from TH analyses, structural analyses based on elastic-plastic-creep analyses are carried out.

## FAILURE EVALUATIONS

According to the NEA reports (Nicolas, 2002) and our previous paper (Katsuyama, 2016), four types of failure criteria as follows are applied in this study;

(1) "Considere" criterion

"Considere" criterion is a stress-based one. The damage variable based on the "Considere" criterion, $D_{cons}$, is defined as Equation 1. If the damage variable, $D_{cons}$, reaches one, the part is judged as failure.

$$D_{cons}(t) = \sigma_{eq}(T(t))/\sigma_{fail}\,(T(t)) \tag{1}$$

where $\sigma_{eq}$ and $\sigma_{fail}$ are Mises equivalent stress and threshold value, which is temperature dependent, respectively. $\sigma_{fail}$ values are reported in the previous paper (Nicolas, 2002).

In this study, a function that $D_{cons}$ is calculated in the area where only tensile stress occurs is introduced in our failure evaluation module, here first principal stress is replaced to $\sigma_{eq}$ in Equation 1, in addition to the conventional function that uses $\sigma_{eq}$ for damage calculation.

(2) Strain criterion

Strain criterion is a strain-based one. The damage variable based on the strain criterion, $D_{strain}$, is defined as Equation 2. If the damage variable, $D_{strain}$, reaches one, the part is judged as failure.

$$D_{strain}(t) = \varepsilon_{eq}(T(t))/\varepsilon_{fail}\,(T(t)) \tag{2}$$

where $\varepsilon_{eq}$ and $\varepsilon_{fail}$ are equivalent strain and threshold value that is set to be 120%, respectively. This value is the same as that is described in the previous paper (Nicolas, 2002).

In this study, a function that $D_{strain}$ is calculated in the area where only tensile stress occurs is introduced in our failure evaluation module, here first principal strain is replaced to $\varepsilon_{eq}$ in Equation 2, in addition to the conventional function that uses $\varepsilon_{eq}$ for damage calculation.

(3) Kachanov criterion

In an evaluation based on the Kachanov criterion, the damage variable due to creep damage, $D_K$, is defined as following equations;

$$D_K = \int_0^t \dot{D}(t)dt \tag{3}$$

$$\dot{D}(t) = \langle \frac{\sigma_{eq}}{A(1-D)} \rangle^R \tag{4}$$

where $\sigma_{eq}$ is the Mises equivalent stress, $A$ and $R$ are material parameters with temperature dependent. $\dot{D}$ corresponds to the rate of damage variable $D_K$. When damage variable $D_K$ reaches one, the part is judged as failure. The parameters of $A$ and $R$ are redefined on the basis of experimental measurements as reported previous papers (Yamaguchi, 2014), (U.S.NRC, 1993). In this study, we do not take the variation of material properties such as Young's modulus and yield strength due to creep damage into account in order to simplify calculation routine and to reduce the calculation time.

In this study, a function that $D_K$ is calculated in the area where only tensile stress occurs is introduced in our failure evaluation module, here first principal stress is replaced to $\sigma_{eq}$ in Equation 4, in addition to the conventional function that uses $\sigma_{eq}$ for damage calculation.

(4) Larson-Miller parameter criterion

Creep failure can be described on the basis of Larson-Miller parameter (LMP) as described following equation;

$$LMP = T\,(C + \log t_{rupture}) \tag{5}$$

where $C$ is a material specific constant, $T$ is the temperature in Kelvin, and $t_{rupture}$ is rupture time. In this study, $C$ is assumed to be 20 and $LMP$ is determined based on the experimental results. It is difficult to evaluate creep rupture by this equation when we consider complicated temperature and pressure distributions due to advances of the debris relocation. Therefore, we establish a creep damage evaluation method based on LMP in the previous paper (Katsuyama, 2016). Using residual lifetime, $t_R$, and increment time, $\Delta t_i$, variation of damage variable, $\Delta D_{LMP,i}$, for each increment, $i$, is calculated by Equation (6). And then, damage variable, $D(t_i)$, for each increment is obtained by Equation (7) as summation of $D(t_{i-1})$ and $\Delta D_{LMP,i}$.

$$\Delta D_{\mathrm{LMP},i}(t) = \Delta t_i / t_R \tag{6}$$

$$D(t_i) = D(t_{i-1}) + \Delta D_{\mathrm{LMP},i}(t) \tag{7}$$

The parameters for LMP criteria are determined by experimental measurements reported by separate papers (Yamaguchi, 2014), (U.S.NRC, 1993).

In this study, a function that $D_{LMP}$ is calculated using the first principal stress in the area where only tensile stress occurs is introduced in our failure evaluation module in addition to the conventional function that uses Mises equivalent stress for damage calculation.

## ANALYSIS MODELS AND METHODS

To estimate leakage start time and location of rupture due to heating by molten pool (the relocated debris), coupled analysis of TH and structural analyses is performed. In this section, the methodology of the analysis is explained.

### Thermal-Hydraulics Analysis

The model used for TH analysis is shown in Figure 1. The model is 1/8 model considering symmetry of lower head and configuration of control rod guide tubes. It is composed of tetra mesh and number of elements is 1,627,236. In the figure, difference of color indicates the difference of the materials as shown in table 1, i.e. green, yellow, and pink are the low alloys steel, stainless steel, and nickel-based alloy, respectively, and the region drawn by sky blue composed of the air and molten pool. Each material property is temperature dependent as listed in tables 2 to 5 (For example U.S.NRC, 1993). For the material properties of Type 308 stainless steel (SS), those of Type 304 SS were applied since there are no significant data. The depth of molten pool and location of internal heat generation can be arbitrarily set considering the situation of assumed accident. Boundary conditions for heat transfer with 22 $^{o}$C of outside temperature are applied to surfaces of lower head, guide tube, stub tubes, and shroud support. The pressure boundary of $1.0\times10^6$ [Pa] are also applied to the top of sky blue region. To consider the phase transformation from solid to liquid, the specific heat between solidus and liquidus line temperatures (2650[K] and 3123 [K], respectively) is set.

In this study, to investigate the influence from difference of accident conditions on time and location of RPV lower head rupture, we assume several patterns with different molten pool depth and location of internal heat generation. For depths of molten pool, 0.29 [m] and 0.58 [m] are assumed, here

0.58 [m] case corresponds to that around 10% of reactor core is melted and relocated to vessel lower head. Heat generation location may depend on the situation of relocated molten core in lower head. If molten core with small particle size fell into the lower head filled with the water in the early stage of accident, the crusts should be formed near the surface of the lower head, and as a result, the upper part of the debris becomes the heat generation location. On the other hand, if large-scale relocation occurs from the early stage of accident, it can be considered that large size of the molten core fell to the lower head, and then the top surface will be cooled by the water remaining in the lower head, the bottom part of the debris becomes the heat generation locations. From such considerations, we assume two cases with different locations of internal heat generation, i.e. center of heat generation locations exist at the top and bottom in the molten pool. If the crust formed, it may act as a thermal insulator. However, in this analysis such adiabatic effect of the crust is not taken into account. Initial condition assumed in this study is that the coolant water in the reactor is completely evaporated (dried condition). We, therefore, set 22 $^{o}$C for structural materials and 100 $^{o}$C for the molten pool and air within the lower head as initial conditions. Internal heat generation of $1.0\times10^{6}$ [W/m$^{3}$] is taken into account. It should be noted that this scenario is different from that of 1F.

Temperature distributions in RPV and its skirt, control rod guide tubes, and stub tubes calculated by the TH analysis is applied to structural analysis.

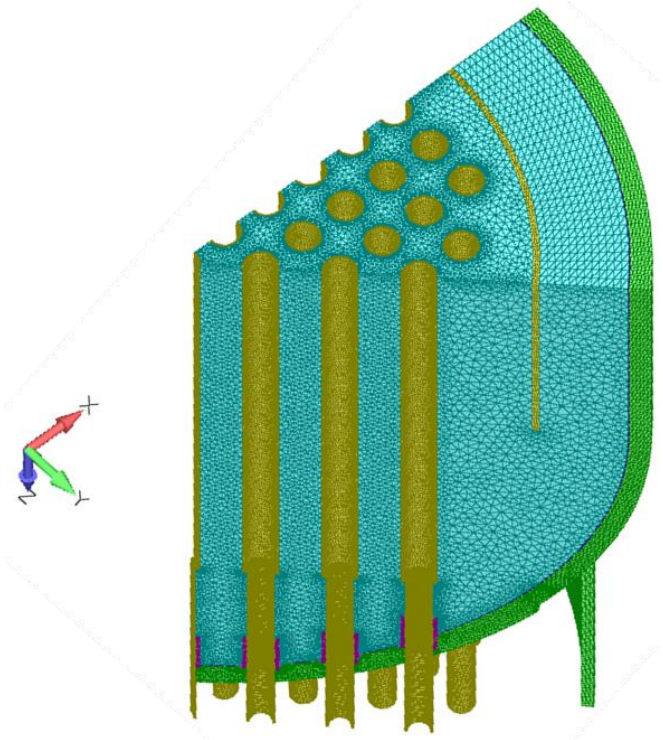

Figure 1. Analysis model for TH analysis.

Table 1: Construction and materials.

| | |
|---|---|
| Lowe head, Skirt | A533B |
| Clad on the inner surface of lower head | Type 308 SS* |
| Control rod guide tube | Type 304 SS |
| Stub tube, Welds | Alloy 600 |

* The same material properties as Type 304 SS are used.

Table 2: Material properties for SA533B.

| | |
|---|---|
| Density [kg/m3] | 7757.87 |
| Specific heat [J/(Kg·K)] | $2.3458838\times10^{-6}\times T^3-0.0037950373\times T^2+2.4088197\times T-7.9739914$ (295.48≦T≦1003.87[K]) |
| Heat transfer coefficient [W/(m·K)] | $3.7479907\times10^{-8}\times T^3-8.8371969\times10\text{-}5\times T^2+0.031768762\times T+49.339687$ (317.67≦T≦1005.76[K]) |

Table 3: Material properties for Type 304 SS.

| | |
|---|---|
| Density [kg/m3] | 7683.71 |
| Specific heat [J/(Kg·K)] | $-9.8016317\times10^{-5}\times T^2+0.29517058\times T+329.68192$ (303.26≦T≦1376.09[K]) |
| Heat transfer coefficient [W/(m·K)] | $0.018896336\times T+7.7956591$ (304.30≦T≦1274.22[K]) |

Table 4: Material properties for Alloy 600.

| | |
|---|---|
| Density [kg/m3] | 8303.18 |
| Specific heat [J/(Kg·K)] | $1.062307\times10^{-14}\times T^6-4.481039\times10^{-11}\times T^5+7.450379\times10^{-8}\times T^4-6.184666\times10^{-5}\times T^3+0.02671917\times T^2-5.41304\times T+822.3227$ (305.15≦T≦1149.32[K]) |
| Heat transfer coefficient [W/(m·K)] | $3.001456\times10^{-6}\times T^2+0.01246358\times T+10.36203$ (318.51≦T≦1151.07[K]) |

Table 5: Material properties for molten pool.

| | |
|---|---|
| Density [kg/m3] | 9,200 |
| Viscosity [Pa·sec] | 1.0E+03 ( T < 2,420 [K] )<br>0.0045 ( T > 2,650 [K] )<br>(Linerly change between 2,420[K] and 2,650[K]) |
| Heat transfer coefficient [W/(m·K)] | 8.0 |
| Solidus temperature [K] | 2,420 |
| Liquidus temperature[K] | 2,650 |
| Latent heat at melting point [J/kg] | 3.52E-05 |
| Specific heat (Solidus temp.) [J/(Kg·K)] | 400 |
| Specific heat (Liquidus temp.) [J/(Kg·K)] | 650 |
| Thermal expansion coefficient [1/K] | 5.0 E-05 |

**Structural Analysis and Creep Damage Evaluation**

We establish three-dimensional model of RPV lower head including control-rod penetrations, stub tubes, J-groove welds, weld-overlay cladding, shroud support, and skirt of RPV as shown in Figure 2. The model is 1/8 model considering symmetry of configuration of control rod guide tubes. Number of elements is 56,943. The materials used in the model are lower alloys steel (ASTM A533B; RPV, skirt),

austenitic stainless steel (Type 316 SS; control rod guide tube, cladding), and nickel based alloy (Alloy 600; stub tube, J-groove weld). Each material property of Young's modulus, Poisson's ratio, yield strength, hardening coefficient after yielding, creep constitutive law is temperature dependent. The details of material properties are the same as previous work (Katsuyama, 2016 Yamaguchi, 2014).

Temperature distribution in each component obtained from TH analysis is applied to this structural analysis on the basis of elastic-plastic-creep analysis. Creep damage evaluations based on "Considere", strain, Kachanov, and LMP criteria are performed by using calculated stress or strain values. In these damage evaluations, two types of calculations were carried out, i.e. one is an improved method that consider only tensile stress (Case 1) and the other is the conventional method based on the equivalent stress or strain that means both compressive and tensile stress are taken into account (Case 2).

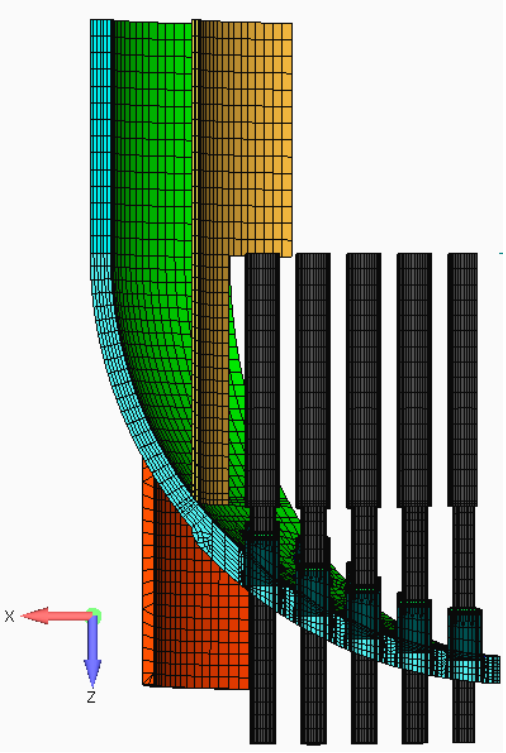


(a) Side view

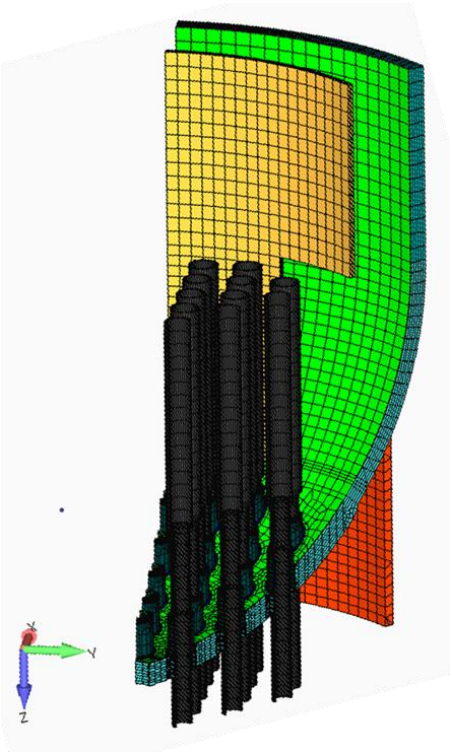


(b) Oblique view

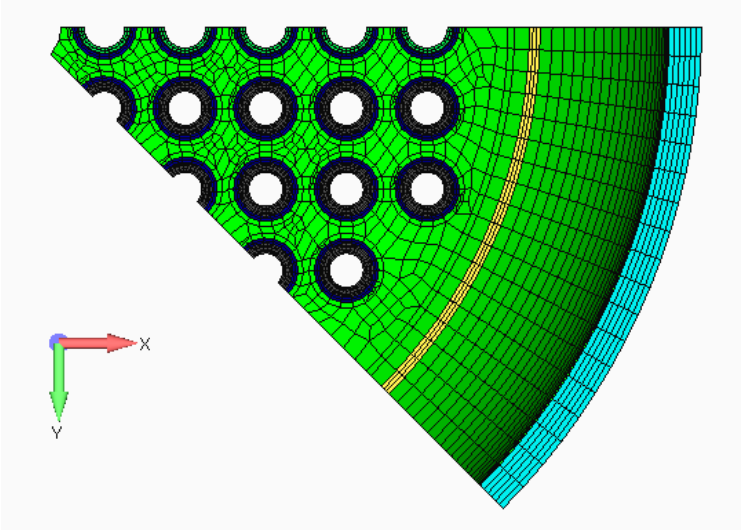


(c) Top view

Figure 2. Analysis model for TH analysis.

## RESULTS AND DISCUSSION

### Thermal-Hydraulics Analysis

Typical analysis results of temperature distributions at lower head due to heating of the relocated molten pool are shown in Figure 3. The time shown in the figure corresponds to the elapsed time from the beginning of internal heating because of evaporation of the coolant water. Figures 3 (a) and (b) show the analysis results with different heat generation locations, i.e. center of internal heat generation location exist at top (a) and bottom (b) in molten pools. If locations of internal heat generation existed at top in molten pool, the maximum temperature is located near the center and upper region in the molten pool (Figure 3 (a)). On the other hand, if locations of internal heat generation existed at bottom in molten pool, the maximum temperature is located near the lower region of molten pool (Figure 3 (b)). The differences of temperature distributions may affect the creep deformation and failure behavior of lower head.

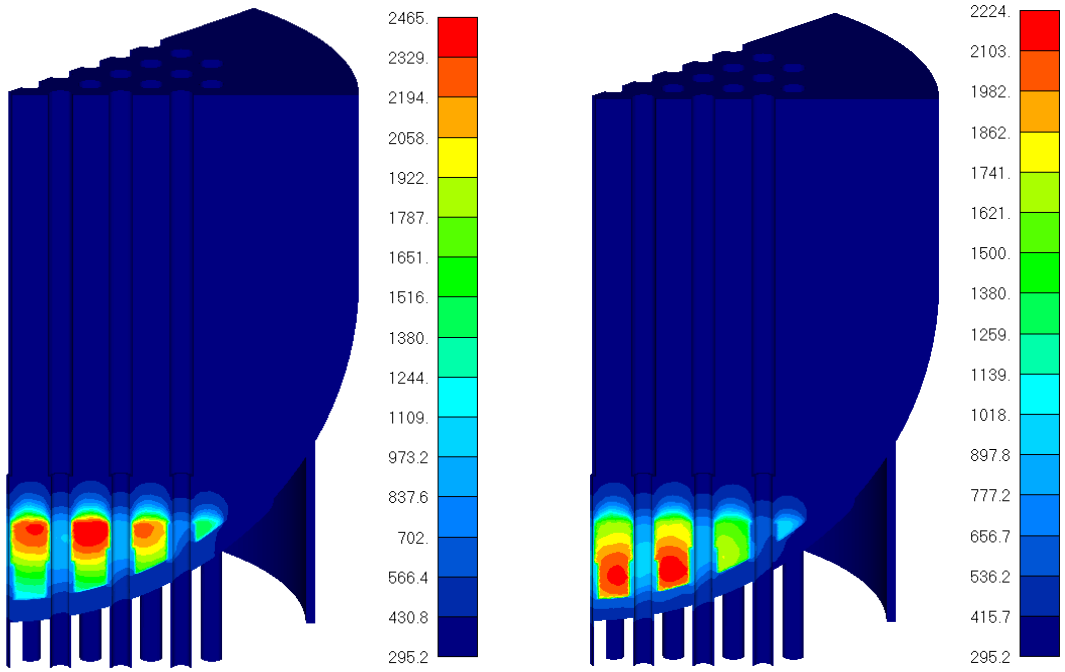


(a) Top (b) Bottom

Figure 3. Temperature distribution at lower head with different heat generation locations, (a) center of heat generation locations exists at the top of the debris, and (b) it exists at the bottom of the debris. (after 10,000 [s]).

### Structural analysis and creep damage evaluation

As described previously, the structural analysis based on elastic-plastic-creep analysis using FINAS/STAR is carried out by applying the temperature distributions in RPV and its skirt, guide tubes, stub tubes and shroud support calculated by TH analysis.

Typical stress distributions obtained from the analyses are shown in Figure 4. Effect of difference in heat generation location on Mises stress distribution is not clearly shown in the figure. It is noted that higher Mises stresses occur within the J-groove welds at the penetrations and within the penetrations at outward of lower head. This fact means that, when we estimate failure behaviors of lower head of BWR due to severe accident, geometrically complicated models including penetrations should be used for failure evaluation.

As examples of analysis results, Figures 5, 6, and 7 represent damage distributions analyzed based on "Considere", Kachanov, and LMP criteria, respectively. In each figure, damage distributions for Cases 1 and 2 are shown in order to compare the results obtained from two types of damage evaluations as described previously. The results of Case 1 obtained by considering only tensile stress, on the other hand, those of Case 2 obtained by both tensile and compressive stresses. Although results from strain criterion are not shown here, there are no regions where are judged to be rupture. From "Considere" criterion, as shown in Figure 5, it is shown that high damaged region is seen at the outer surface of RPV, especially near the center among some penetrations. When compressive stress is also considered, higher damaged regions are also recognized in the stub tubes and control rod guide tubes. From Kachanov criterion, in case that the tensile stress is only considered (Figure 6 (a)), damaged regions where the damage parameters reach unity are seen in not only control rod guide tubes outside of RPV but also J-groove welds jointing stub tubes and guide tubes. From the view point of leakage of the molten core from the RPV, the latter regions are important for the severe accident progressions. If we took the compressive stress into account as well, wider region including stub tubes and guide tubes were judged as rupture. Damage distributions obtained by Kachanov criterion based on both tensile and compressive stresses were similar to those of "Considere" criterion as shown in Figures 5 (b) and 6 (b) but the damage values are different. LMP criterion provides different result from "Considere" and Kachanov criteria, i.e. damaged regions are seen within only the control rod guide tubes.

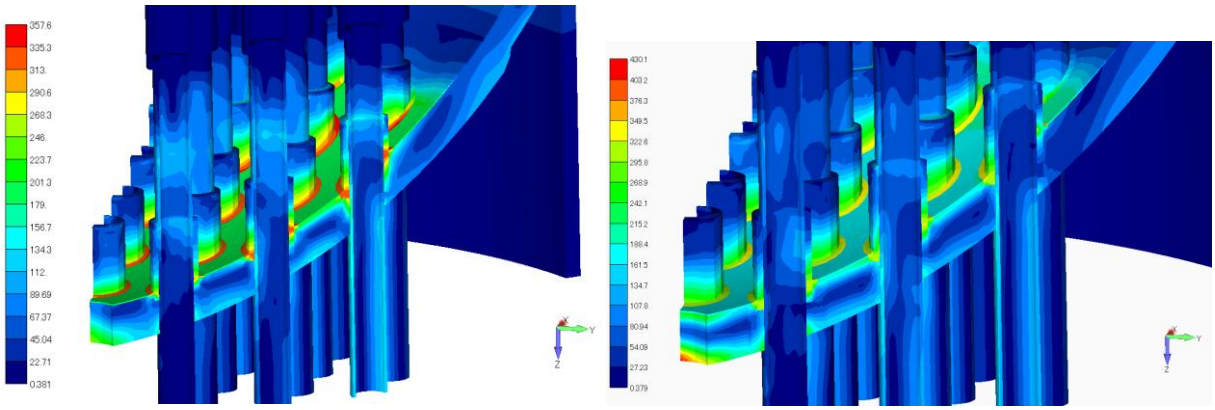

(a) Top (b) Bottom

Figure 4. Mises-equivalent stress distributions at lower head with different heat generation location conditions (Depth = 0.58 [m], at 10,000 [s]).

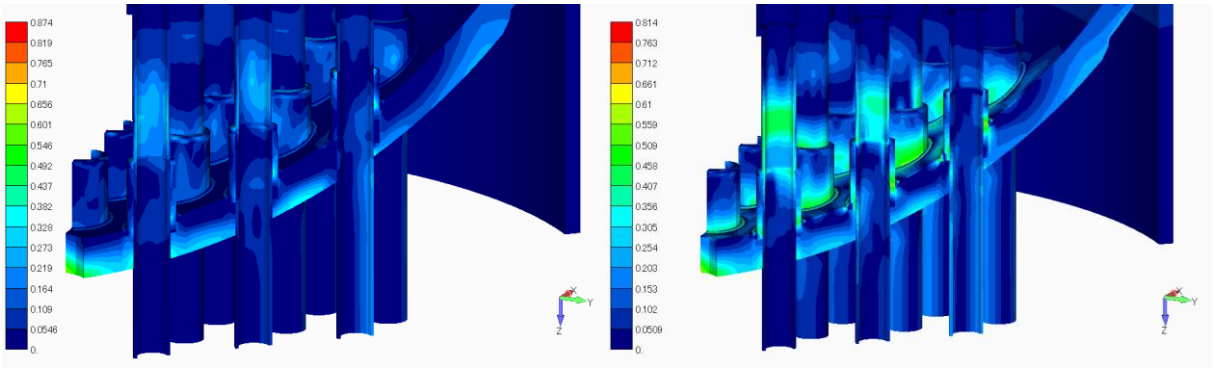

(a) Case 1 (b) Case 2

Figure 5. Damage distribution from "Considere" criterion (at 10,000 [sec], Depth = 0.58 [m], heat gen. point = Top).

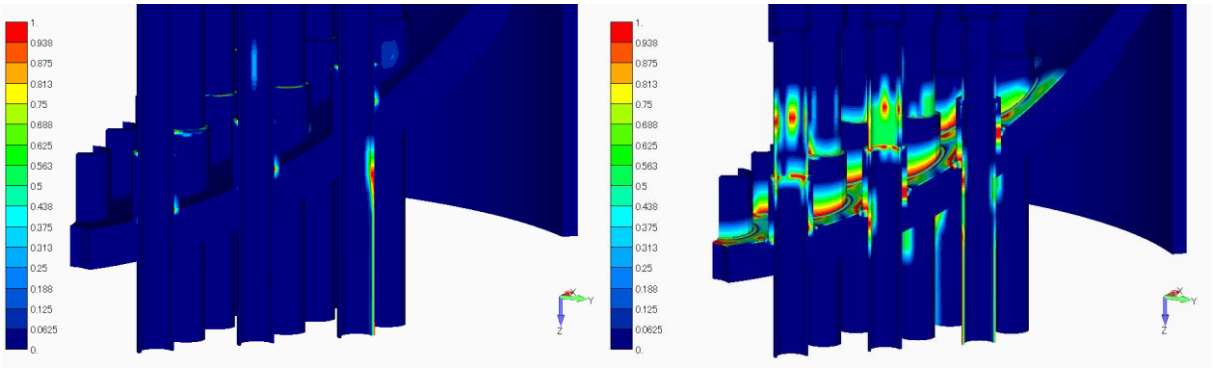

(a) Case 1 (b) Case 2

Figure 6. Damage distribution from Kachanov criterion (at 10,000 [sec], Depth = 0.58 [m], heat gen. point = Top).

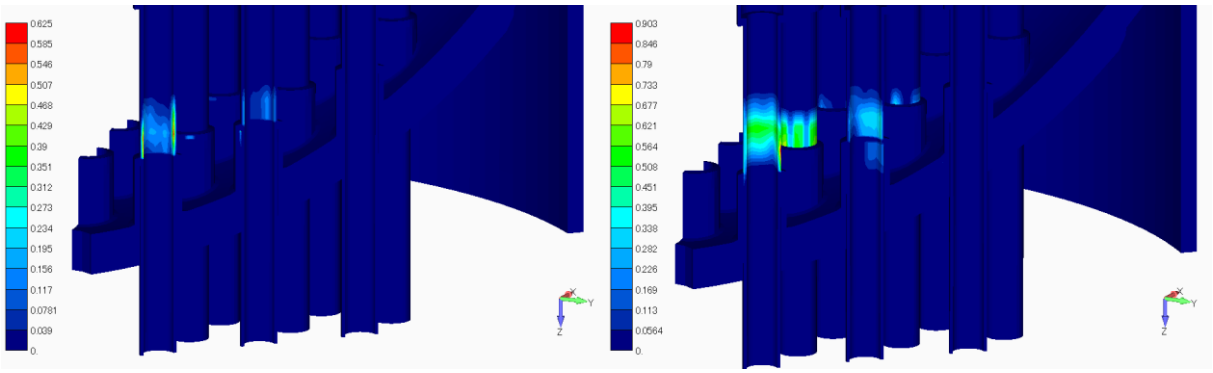

(a) Case 1 (b) Case 2

Figure 7. Damage distribution from LMP criterion (at 20,000 [sec], Depth = 0.58 [m], heat gen. point = Top).

The results obtained from each damage criterion are summarized as following. It is noted that each criterion indicates that rupture of lower head due to heating by the relocated molten core occurs at similar location, i.e. the control rod guide tube penetrations.

(1) Differences from failure criteria

Based on “Considere” criterion evaluation, leakage of molten core from the lower head cannot be recognized because higher damage values were particularly located outside the lower head, especially near the penetrations. From Kachanov damage criterion, in each case, the damage values became one at earlier time compared with the other damage criteria, and leakage paths of molten core from the lower head was formed at the control rod guide tubes, or J-welds between stub tubes and guide tubes. Leakage time and paths differ depending on analysis conditions such as debris depth and heat generation locations, but in most cases molten core flew out from the control rod guide tubes. In the case of LMP criterion, damaged regions can be seen in the control rod guide tubes. Here, when only tensile stress is considered, leakage of molten core does not occur in each case, but when the compressive stress is also considered, leakage paths may be located at the control rod guide tubes. In this case, failure mode of the tubes may correspond to the buckling. However, because significant deformation that causes buckling was not recognized in the analyses, further investigations on improvement of the creep constitution law, etc., are

necessary. Based on strain criterion evaluation, as described previously, there are no regions where are judged to be rupture.

(2) Differences in the debris depth

Damaged regions may move to the mountain side as the debris depth becomes deeper and the leakage start time also becomes shorter when the heat generation location exists at the top of the debris. On the other hand, when the heat generation location exists at the bottom of the debris, there are no significant differences in leakage start time and leakage paths with different debris depth.

(3) Differences of heat generation location

In most cases, except for the case that the debris depth was 0.58 [m] and the both of tensile and compressive stresses were considered in damage evaluations, the leakage start time becomes faster if heat generation location existed at the top of molten pool compared with the case that heating generation location is the bottom part of molten pool. In this case, estimated results indicate that molten core flows out from the guide tubes.

There is a large difference in failure time estimated by each evaluation. Further improvements of evaluation methods are necessary for more accurate assessments of rupture behavior of BWR lower heads.

**SUMMARY**

To assess progress of severe accident and to predict time and location of rupture of BWR lower heads due to severe accident, we developed finite element model of RPV lower head including penetrations and welds, and four types of creep damage failure evaluation methods of “Considere”, strain, Kachanov, and LMP criteria. Through coupled analysis of TH and structural analyses with different the debris depth and heat generation locations, it was shown that failure regions of BWR lower head are only the control rod guide tubes or stub tubes under simulated conditions.

**REFERENCES**

Onizawa K. and Hashimoto K., Three-dimensional thermal stress analyses for the TMI-2 vessel lower head using finite element method, Three mile island reactor pressure vessel investigation project, achievements and significant results (1993), pp. 322-334.

Humphphries L. L. et al., OECD Lower Head Failure Project Final Report (Volume 1 - Integral Experiments and Material Characterization) (2002).

Humphphries L. L. and Smith J., OECD Lower Head Failure Project Final Report (Volume 2 - Numerical Simulation and Modeling) (2002).

Tran C. T., Kudinov P. and Dinh T. N., An approach to numerical simulation and analysis of molten corium coolability in a boiling water reactor lower head, Nuclear Engineering and Design, Vol. 240 (2010), pp. 2148-2159.

Villanueva W., Tran C. T. and Kudinov P., Coupled thermo-mechanical creep analysis for boiling water reactor pressure vessel lower head, Nuclear Engineering and Design, Vol. 249 (2011), pp. 146-153.

Katsuyama J., Yamaguchi Y., Nemoto Y., Kaji Y., and Yoshida H., Development of failure evaluation method for BWR Lower head in severe accident; - Creep damage evaluation based on thermal-hydraulics and structural analyses -, Mechanical Engineering Journal Vol. 3 (2016) Paper No.15-00682..

ITOCHU Techno-Solutions Corporation, FINAS/CFD theoretical manual, Ver. 2013 (2013). (in Japanese)

ITOCHU Techno-Solutions Corporation, FINAS/STAR theoretical manual, Ver. 2013 (2013). (in Japanese)

Nicolas L. and Locatelli T., Failure propagation simulation in a RPV lower head under severe accident loading conditions, OLHF Seminar, Madrid June 2002 (2002).

U.S.NRC, "Light Water Reactor Lower Head Failure Analysis," NUREG/CR-5642 (1993).

Yamaguchi Y., Katsuyama J., Kaji Y., Yoshida H., and Li Y., Development of Failure Evaluation for BWR Lower Head in Severe Accident; (1) High Temperature Creep Test and Creep Damage Model, Proceedings of ICONE-23, ICONE23-1533 (2015).

Marsden, B. J. and Hall, G. N. (2012). "Graphite in Gas-cooled Reactors," *Comprehensive Nuclear Materials*, Elsevier, UK.

Cook, R. D., Malkus, D. S., Plesha, M. E. and Witt, R. J. (2002). *Concepts and Applications of Finite Element Analysis, 4th ed*., John Wiley & Sons.

Prinja, N. K., Shepherd, D., Curley, J. (2005). "Simulating structural collapse of a PWR containment," *Nuclear Engineering and Design*, UK, 230 2033-2043.

Hughes, T. J. R. and Allik, H. (1969). "Finite Elements for Compressible and Incompressible Continua," *Proc., Symposium on Application of Finite Element Methods in Civil Engineering*, ASCE, Nashville, TN, 27-62.

International Conference of Building Officials. (1988). *Uniform Building Code*. Whittier, California, USA.